

A new energy-based ground motion selection and modification method limiting the dynamic response dispersion and preserving the median demand

*Original*

A new energy-based ground motion selection and modification method limiting the dynamic response dispersion and preserving the median demand / Marasco, Sebastiano; Cimellaro, G. P.. - In: BULLETIN OF EARTHQUAKE ENGINEERING. - ISSN 1570-761X. - (2018), pp. 1-21. [10.1007/s10518-017-0232-5]

*Availability:*

This version is available at: 11583/2685798 since: 2019-10-16T15:35:31Z

*Publisher:*

Springer Netherlands

*Published*

DOI:10.1007/s10518-017-0232-5

*Terms of use:*

This article is made available under terms and conditions as specified in the corresponding bibliographic description in the repository

*Publisher copyright*

Springer postprint/Author's Accepted Manuscript

This version of the article has been accepted for publication, after peer review (when applicable) and is subject to Springer Nature's AM terms of use, but is not the Version of Record and does not reflect post-acceptance improvements, or any corrections. The Version of Record is available online at: <http://dx.doi.org/10.1007/s10518-017-0232-5>

(Article begins on next page)



42 the fundamental period of the structure (with 5% damping ratio) is the most commonly used IM  
 43 parameter. In these cases, selection of records is based on the mean compatibility between the  
 44 response spectrum and the target spectrum. The dispersion between the elastic and target response  
 45 spectra has been taken into account by many researchers. Ambraseys et al. [4] suggested the  
 46 verification of the spectral compatibility of a certain record according to the parameter reported in  
 47 Equation (0).

$$48 \quad D_{ms} = \frac{1}{N} \sqrt{\sum_{i=1}^N \left( \frac{Sa_o(T_i)}{PGA_o} - \frac{Sa_s(T_i)}{PGA_s} \right)^2} \quad (0)$$

49 where  $N$  is the number of periods within the reference interval and  $Sa_o(T_i)$  is the spectral acceleration  
 50 of the record at period  $T_i$ .  $Sa_s(T_i)$  is the target spectral acceleration at the same period value, and  $PGA_o$   
 51 and  $PGA_s$  are the peak ground acceleration of the considered record and of the target, respectively.  
 52 In addition, Iervolino et al. [5] reported the mean deviation of the record's spectra with respect to the  
 53 target spectrum in a specific period range (Equation (0)).

$$54 \quad D_i = \sqrt{\frac{1}{N} \sum_{i=1}^N \left( \frac{Sa_j(T_i) - Sa_s(T_i)}{Sa_s(T_i)} \right)^2} \quad (0)$$

55 Here, the  $PGA$  value is not taken as a normalizing factor and  $Sa_j(T_i)$  represents the spectral  
 56 acceleration of the  $j^{\text{th}}$  record at period  $T_i$ . The methodology proposed by Iervolino et al. [5] has been  
 57 implemented in the REXEL software.

58 Bradley [6] proposed a ground motion selection procedure based on the generalized conditional  
 59 intensity measure (GCIM) approach. The method is applied by using random realizations from the  
 60 conditional multivariate distribution of intensity measures derived by the GCIM approach. This  
 61 method allows to select natural, synthetic and simulated motions considering any number of IM  
 62 assumed as important parameters in the dynamic structural response assessment.

63 On the other hand, the scenario-based assessment is performed considering the source-to-site  
 64 distance, faulting system, soil category, and earthquake magnitude. Shome et al. [7] picked real  
 65 accelerograms built upon the basis of four different magnitude-distance pairs ( $M$ - $R$ ), restricting the  
 66 variation in the target values. Previous research has failed to come up with an efficient  $M$ - $R$  based  
 67 procedure for the structural dynamic response. Baker and Cornell confirmed [8] that the source-to-  
 68 site distance is not statistically of great importance to the response of the structure. On the other hand,  
 69 they reported that earthquake magnitude is a key factor. It is worth noting that if soil response or  
 70 liquefaction analyses are to be performed, the soil profile characteristics must be integrated in the  
 71 selection process. In these cases, the cyclic action of the motion influences the response of the soil.  
 72 Thus, the aim is to achieve a set of accelerograms that do not have significant gaps in the Fourier  
 73 Amplitude Spectrum (FAS) and in the duration. The selection procedure has to be carried out  
 74 considering a full classification of the site in terms of shear wave velocity at the uppermost 30 m  
 75 ( $V_{S,30}$ ) and the magnitude that influences the duration of the ground motion.

76 The performance of a structure subjected to a dynamic excitation is strongly dependent on the  
 77 frequency content of the input. Thus, the comparison of the energy content of the motions with the  
 78 target energy content represents a new approach focused on the minimization of the structural  
 79 response dispersion and accuracy in the mean dynamic response prediction. In addition, the ground  
 80 motion scaling is performed to have similar severity that produces a comparable structural damage.  
 81 In the context of performance-based design, the proposed GSM methodology ensures a suitable  
 82 approach to assess the dynamic response of a structural and geotechnical system.

83 Further details on the proposed methods are given in section 2 including the novelty and benefits of  
 84 the method. A case study illustrating application of the method for a steel building is presented in  
 85 paragraph 3. In addition, a second case study is presented in paragraph 4. In the latter, a reinforced  
 86 concrete pier bridge is investigated, using the software OPENSIGNAL 4.1 [9] for the GSM  
 87 procedure.

88 **2 DESCRIPTION OF THE METHOD**

89 A novel GSM procedure for minimizing the dispersion of the Engineering Demand Parameters  
90 (EDP) and enhancing the accuracy in the prediction of dynamic structural response is proposed. The  
91 estimation in the response of the structural system subjected to a seismic action is affected by the  
92 uncertainty in the ground motion selection and in the dynamic response of the structure. The  
93 uncertainty in the ground motion selection for a given site may be reduced considering a range of  
94 magnitude and source-to-site distance (such as source-to-site distance). Moreover, the variability of  
95 the waveform characteristics of the input affects the estimation of the fragility functions. The  
96 proposed method allows to select ground motions having a limited variance of waveform  
97 characteristics such as peak parameters and input energy content parameters. Reducing the record-to-  
98 record variability enhances the estimation of the dynamic structural response and its fragility [10].  
99 In fact, the seismic response dispersion, and its accuracy, is strongly correlated to parameters  
100 describing the seismic input. The natural records are selected in order to have a similar intensity  
101 measure and a low record-to-record variability. Therefore, the selected set of motions produce a  
102 structural dynamic response that reflects the median demand with a reduced dispersion.  
103 In the structural assessment process, the increase in accuracy leads to a better estimation of the  
104 aftermath consequences.  
105

106 *2.1 Selection of the target spectrum*

107  
108 Finding the target spectrum is the first step in the selection procedure. One target spectrum that is  
109 widely used is the Uniform Hazard Spectrum (UHS). This comes from the PSHA [2] and defines the  
110 locus of spectral acceleration at each period having a given exceedance probability. Ground motions  
111 with different magnitudes and source-to-site distance values contribute to the total hazard. One of the  
112 observed key differences is that near-source earthquakes control the high frequency part of the UHS,  
113 while distant earthquakes influence low frequency. The UHS is not representative as target spectrum  
114 for any individual seismic excitation because no single earthquake will produce a response in a wide  
115 range of frequency content. This in turn draw attention to the Conditional Mean Spectrum (CMS- $\epsilon$ )  
116 that is obtained conditioning on a spectral acceleration at only one period according to commonly  
117 used de-aggregation parameters  $M$ ,  $R$  and  $\epsilon$  [8][11]. The last parameter is a measure of the difference  
118 between the mean logarithmic spectral predicted demand and the logarithmic spectral acceleration of  
119 a record with a predefined attenuation model for the site of interest. Baker and Cornell [8] looked into  
120 the dynamic response of a Multi Degree Of Freedom (MDOF) system taking into account the ground  
121 motion records having a specific intensity and matching UHS and CMS- $\epsilon$ . The selected records that  
122 are based on the CMS- $\epsilon$  generated less dispersion in the dynamic response of structures.  
123

124 *2.2 Ground motion scaling*

125  
126 Typically, the spectral acceleration at reference period ( $S_a(T_{ref})$ ) is the intensity measure parameter  
127 (IM) used in the ground motion selection approach. This measure provides information on the  
128 maximum elastic seismic action on the structure. For MDOF structural systems, the reference period  
129  $T_{ref}$  may be taken equal to the first mode ( $T_1$ ). This is because the dynamic response of the system is  
130 dominated by the first mode. In such a case when the stiffness and the mass of the structural system  
131 are non-uniformly distributed, the dynamic response is computed as a combination of the different  
132 modes. A modal participation factor with a value greater than 85% in both directions is recommended.  
133 In these cases, the reference period may be derived from weighted arithmetic mean of the periods  
134 corresponding to the investigated modes with modal participation factors (Equation (0)).

135

$$T_{ref,h} = \frac{\sum_{i=1}^N T_{i,h} \cdot |g_{i,h}|}{\sum_{i=1}^N |g_{i,h}|} \quad (0)$$

136 where  $T_i$  and  $g_i$  represent the  $i^{th}$  mode's period and modal participation factor, respectively, while  $h$   
 137 index is related to the horizontal motion component. The amount of the real ground motion records  
 138 that are freely accessible is not sufficient to have a great number of motions having identical spectral  
 139 acceleration at the same period. It is essential to modify the records to have multiple sets of compatible  
 140 ground motions. Most of the existing modification procedures are based on scaling the spectral  
 141 acceleration at reference period ( $S_{a,i}(T_{ref})$ ) to the target spectral acceleration ( $S_{a,TS}(T_{ref})$ ) (Equation (0)  
 142 ). This approach considers records resulting in the same maximum elastic seismic action on the  
 143 structure.

144

$$SF_{I,i} = \frac{S_{a,TS}(T_{ref})}{S_{a,i}(T_{ref})} \quad (0)$$

145 In the proposed methodology, each record is adjusted in two parallel ways. Equation (0) is used to  
 146 carry out the first modification approach, while the second modification method is based on the  
 147 Housner intensity of the motion within the considered range of period.  
 148 Housner intensity is evaluated for every record in the range  $\Delta T = 0.2 \cdot T_{ref} \sim 2 \cdot T_{ref}$  ( $I_{H,i}(\Delta T)$ ) which is the  
 149 interval period in which the mean spectrum-compatibility has to be validated. Pseudo Velocity  
 150 Spectrum ( $PVS$ ) is used to calculate the target Housner intensity ( $I_{H,TS}(\Delta T)$ ). Equation (0) shows the  
 151 Housner intensity-based scale factor of the  $i^{th}$  record.

152

$$SF_{II,i} = \frac{I_{H,TS}(\Delta T)}{I_{H,i}(\Delta T)} \quad (0)$$

### 153 2.3 Ground motion selection

154

155 The selection method depends on the energy content of the ground motion in the different frequency  
 156 bands. It is well known that the energy of the periodic signal is proportional to its squared amplitude.  
 157 As indicated by Fourier, a generic time history can be decomposed in infinite harmonic periodic  
 158 functions with given amplitude ( $A_i$ ) and circular frequency ( $\omega_i$ ). The Fourier transform provides  
 159 indication in the amplitude contribution for every frequency of the ground motion. The Fourier series  
 160 is used to calculate the trend of the squared amplitude ( $A_i^2$ ) in the frequency domain. The frequency  
 161 domain is sampled in different bands ( $\Delta f$ ) of 0.5 Hz. In addition, the total energy-proportional  
 162 coefficient is evaluated for every  $\Delta f$  as the summation of each contribution in the given frequency  
 163 band. The amplification function ( $/A/$ ) is used to calculate the target energy content as the ratio  
 164 between the spectral acceleration at the period under consideration and the period corresponding to  
 165  $T=0$  ( $PGA$ ). The CMS- $\varepsilon$  for the given site has been selected as target spectrum and sampled in  
 166 intervals  $\Delta T=0.05$  s and the amplification function corresponding to the generic  $i^{th}$  period is given by  
 167 (Figure 1.a).

168

$$|A_i| = \frac{S_{a,TS}(T_i)}{S_{a,TS}(T=0)} = \frac{S_{a,TS}(T_i)}{PGA_{TS}} \quad (0)$$

169 where  $S_{a,TS}(T_i)$  represents the target spectral acceleration at the generic period  $T_i$ , while  $PGA_{TS}$  is the  
 170 target peak ground acceleration.

171 According to the definition of the amplitude function and by setting a damping ratio  $\xi$  equal to 5%,  
 172 the exciting target frequency ( $\omega_{f,i}$ ) is computed (Equation (0)).

173

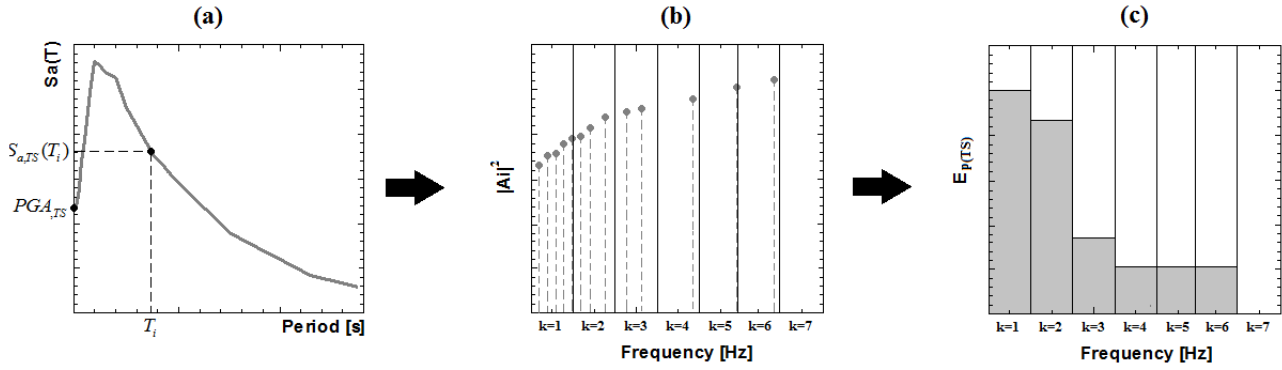
$$|A_i| = \frac{1}{\sqrt{\left(1 - \left(\frac{\omega_{f,i}}{\omega}\right)^2\right)^2 + \left(2 \cdot \xi \cdot \frac{\omega_{f,i}}{\omega}\right)^2}} \quad (0)$$

174 Then the terms  $|A_i|^2$  and  $\omega_{f,i}$  are determined by repeating the same approach for each sampled period  
 175 (Figure 1.b). The target percentage energy content is acquired by splitting the frequency domain into  
 176 multiple bands of  $0.5\text{Hz}$  and then aggregating their contributions. For the  $k^{\text{th}}$  frequency band, the  
 177 target percentage energy contribution ( $E_{p,k}(TS)$ ) is given by Equation (0) (Figure 1.c).

178

$$E_{p,k}(TS) = \frac{\sum_{\Delta f_k=0.5\text{Hz}} (|A_k|)^2}{\sum_{k=1}^N (|A_k|)^2} \quad (0)$$

179 where  $\sum_{k=1}^N (|A_k|)^2$  represents the total energy-proportional coefficient in the frequency domain that is  
 180 sampled in  $N$  total bands.



181

182 Figure 1. Scheme of the procedure used to obtain the target energy content in the discretized  
 183 frequency domain. (a) Discretization of the period domain, calculation of the amplification function  
 184 and evaluation of the associated frequencies, (b) definition of the distribution of  $(|A_i|)^2 - \omega_{f,i}$  and (c)  
 185 target energy-proportional coefficient for each  $k^{\text{th}}$  frequency band.

186

#### 2.4 Summary of the methodology

187

188 Scaling and selection procedure is summarized in the following steps:

- 189 1) Set a maximum and a minimum value for the  $SF_I$  and select all the records in such a way to be  
 190 within the interval  $SF_{I(min)} - SF_{I(max)}$ .
- 191 2) A maximum absolute percentage dispersion of the PGA ( $\sigma_{PGA}$ ) with respect to the target PGA is  
 192 assigned. This step allows to minimize the PGA variance of the records for a given hazard  
 193 scenario.
- 194 3) Maximum and minimum values are set for the moment magnitude and the source-to-site distance  
 195 according to the de-aggregation study of the site. This permits to select significant records within  
 196 the seismicogenic characteristics of the selected site.
- 197 4) The Housner intensity-based scale factors are evaluated for the modified ground motion ( $SF_{II}$ ).  
 198 Thus, only ground motions matching the target Pseudo Velocity Spectrum (PSV) in the selected  
 199 period range are considered.
- 200 5) The selection is carried out considering the ground motion having equal values for  $SF_I$  and  $SF_{II}$ .  
 201 Since the number of motions available in the strong motion database is reduced, a small variance  
 202 between the two values of the scale factors ( $\sigma_{SF}$ ) has to be fixed. Thus, the ratio between the two  
 203 scale factors must be limited in the range given by Equation (0).

204

$$(1 - \sigma_{SF}) \leq \frac{SF_{I,i}}{SF_{II,i}} \leq (1 + \sigma_{SF}) \quad (0)$$

205

Generally a variance value less than 15% is suggested.

206

6) Preliminarily, only records satisfying the conditions mentioned in steps 2, 3, and 5 are selected (compatible records).

207

208

7) Finally, only seven records have to be selected (in both horizontal directions for structural analysis, and in a single horizontal direction for soil response analysis). The selection procedure is performed comparing the energy content of each compatible record with the target energy content. For a general compatible record, the energy trend coefficient ( $C_E$ ) is computed as in Equation (0).

209

210

211

212

213

$$C_E = \frac{1}{\left\{ |E_{p,k(i)} - E_{p,k(TS)}| \cdot \left[ \sum_{j=1}^{20} |E_{p,k(i)} - E_{p,k(TS)}| \right] \right\}} \quad (0)$$

214

where  $E_{p,k(i)}$  and  $E_{p,k(TS)}$  represent the total energy percentage content for the  $k^{\text{th}}$  frequency band of the  $i^{\text{th}}$  record and of the target, respectively. The summation in the denominator indicates the total dispersion of the energy content of the  $i^{\text{th}}$  record with respect to the target.

215

216

217

For every frequency band, all the records are arranged in a descending order of  $C_E$  values. Typically, the frequency components of a seismic signal are contained between 0.1 and 10 Hz. Considering the maximum frequency threshold as 10 Hz and assuming a frequency band amplitude of 0.5 Hz, the total number of frequency bands to be analyzed are 20. Therefore, the summation expressed in Equation (0) is performed for 20 different frequency bands.

218

219

220

221

222

As indicated by the percentage contributions of energy band content, a number  $n_k$  of records is chosen for every band so as to have the greater values for the energy trend coefficient. This strategy begins from  $\Delta f$ : 0-0.5Hz and is halted when the number  $\sum_{k=1} n_k$  accomplishes a value of 7.

223

224

225

## 2.5 Advantages of the methodology

226

227

a) Spectral acceleration-based selection procedures are somehow problematic because the PGA may not be close in value to the PGA derived from the hazard analysis. One reason could be the inadequacy of the spectrum compatibility within the low periods range. In addition, a large variance of the PGA of a records group may create high dispersion of the maximum dynamic response of the structure. Nevertheless, the variation can be limited by assigning a maximum absolute dispersion for the PGA ( $\sigma_{PGA}$ ) with respect to the target.

228

229

230

231

232

233

234

b) The initially proposed modification method is used in other GSM procedures. Every scaled record generates identical maximum elastic actions on the structure. To avoid distortion in the frequency and energy content, the maximum and minimum scale factor limits ( $SF_{I(min)}$  and  $SF_{I(max)}$ ) have to be assigned. The ratio between the scale factor based on the reference spectral acceleration and on the Housner intensity does not to exceed the value of  $1 \pm \sigma_{SF}$ . This is equivalent to expect constant values of Housner intensity as well as to generate similar elastic seismic action on structure. The Housner Intensity correlates the severity of seismic events with building structural damage. Thus, each adjusted record generates an approximately similar structural damage. Furthermore, the equal Housner intensity allows controlling the average trend of the  $PSV$  and then the acceleration response spectrum for every record. The selected records have the maximum energy content representativeness with the target energy distribution. Furthermore, the consistency of the  $PGAs$  with the relative hazard value makes the peak amplitude of the records quite similar. Therefore, the proposed selection procedure has the potential to

235

236

237

238

239

240

241

242

243

244

245

246

247 influence and control the energy input of the structure. This in turns provides a group of motions  
248 with a contained variance in the seismic energy content (e.g. Arias Intensity).

249  
250 c) Tso et al. [12] claimed that the energy and frequency content of a ground motion are associated  
251 with the ratio between the peak value of acceleration and peak value of velocity (*AV* ratio). After  
252 analyzing 45 records, three classes of *AV* ratio were identified (low, intermediate, and high).  
253 Records of a given group have shown a similar trend in terms of energetic content in the frequency  
254 domain. Since the records selected have moderate variability of energetic contents in frequency  
255 domain, each of them assume a small variability of *AV* ratio.

256  
257 d) Structural damage caused by seismic activities is proportional to the number (*n*) and amplitude  
258 (*m*) of the plastic load-unload cycles. Manfredi and Cosenza [13] proposed an index for structural  
259 damage (*I<sub>D</sub>*) through the Arias intensity (*I<sub>A</sub>*), *PGA*, and *AV* ratio (Equation (0)).

$$260 \quad I_D = \frac{2 \cdot g}{\pi} \cdot \frac{I_A}{PGA^2} AV \quad (0)$$

261 Equation (0) reports the ground motion hysteretic energy demand (*E<sub>H</sub>*) as damage severity  
262 parameter.

$$263 \quad E_{h,d} = F_y \cdot (\Delta u_{max} - \Delta u_y) \cdot [1 + m \cdot (n - 1)] \quad (0)$$

264 where *m* and *n* are directly proportional to *I<sub>D</sub>*. The parameters *F<sub>y</sub>* and *Δu<sub>y</sub>* identify the yielding  
265 action and displacement, respectively. These terms are related to the structure and they are  
266 independent of any external agents, while *Δu<sub>max</sub>* is the maximum dynamic response in terms of  
267 displacements.

268 The low variability of the *PGA*, *AV* ratio, damage severity (expressed by means of the hysteretic  
269 energy demand *E<sub>H</sub>*), and Arias intensity (*I<sub>A</sub>*) prompts a controlled dynamic response of the  
270 structure (*Δu<sub>max</sub>*). The dynamic response of multi-story buildings can be alternatively expressed  
271 as the sum of drift contribution at each story ( $\sum_i \Delta u_{max,i}$ ). The proposed GSM procedure ensures

272 a maximum control over the story drift, obtaining low dispersion among the seven selected  
273 records and an accurate expected response for a given IM, as indicated in Equation (0).

### 274 3 CASE STUDY 1

#### 275 3.1 Description of the structure and structural analysis

276  
277 The case study is a five-story steel hospital in the city of Oakland, California, US (Lat: 37.7792,  
278 Long: -122.1620). Non-linear dynamic analyses have been performed through the structure. The  
279 lateral resisting system is a dual system (moment resisting frames and braces in both directions).  
280 Beams and columns have H sections, while hollowed structural section (HSS) have been assigned to  
281 the braces. The software Sap2000 [14] has been used to build the FEM model of the studied structure  
282 (Figure 2).

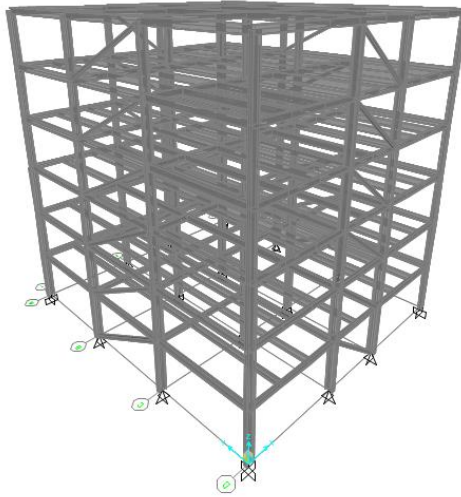


Figure 2. FEM extruded model of the case study building.

283  
284

285

286 Concentrated plasticity model (FEMA 356 type P-M2-M3 for columns and M2-M3 for beams) has  
287 been chosen to account for the nonlinearity in the structural components. As for the bracing system,  
288 axial hinges have been allocated. A 3% damping ratio has been assigned to the frames according to  
289 Rayleigh formulation. Nonlinear direct integration has been used to perform the analysis. The analysis  
290 has been performed taking into consideration the P- $\Delta$  effects and applying the horizontal acceleration  
291 time histories in the two principal plan directions of the building model.

### 292 3.2 Ground motion selection and modification

293

294 Seven hazard levels (HL) have been analyzed (i.e., 75%, 60%, 50%, 20%, 10%, 5% and 2% of  
295 exceedance probability in 100 years). The mean value of the epicenter distance ( $R_{mean}$ ), the  
296 logarithmic spectral offset at reference period ( $\varepsilon(T_{ref})$ ), and the moment magnitude ( $M_{W,mean}$ ), have  
297 been computed according to Boore-Atkinson attenuation model [15]. Further detail on the data can  
298 be found in the interactive de-aggregation of USGS (<http://geohazards.usgs.gov/deaggint/2008/> )  
299 [16]. The shear wave velocity at the uppermost 30 m has been assumed equal to 736 m/s according  
300 to the Global Vs30 Map Server (<http://earthquake.usgs.gov/hazards/apps/vs30/>) [16]. The  
301 Conditional Mean Spectrum acquired from the de-aggregation study (CMS- $\varepsilon$ ) has been taken as the  
302 target spectrum [17][1] and the model of Baker and Jayaram [18] has been considered as correlation  
303 model. OPENSIGNAL 4.1 software [9] has been used to define CMS- $\varepsilon$  for each HL. Table 1 displays  
304 the values of the IM parameters and PGA for each HL.

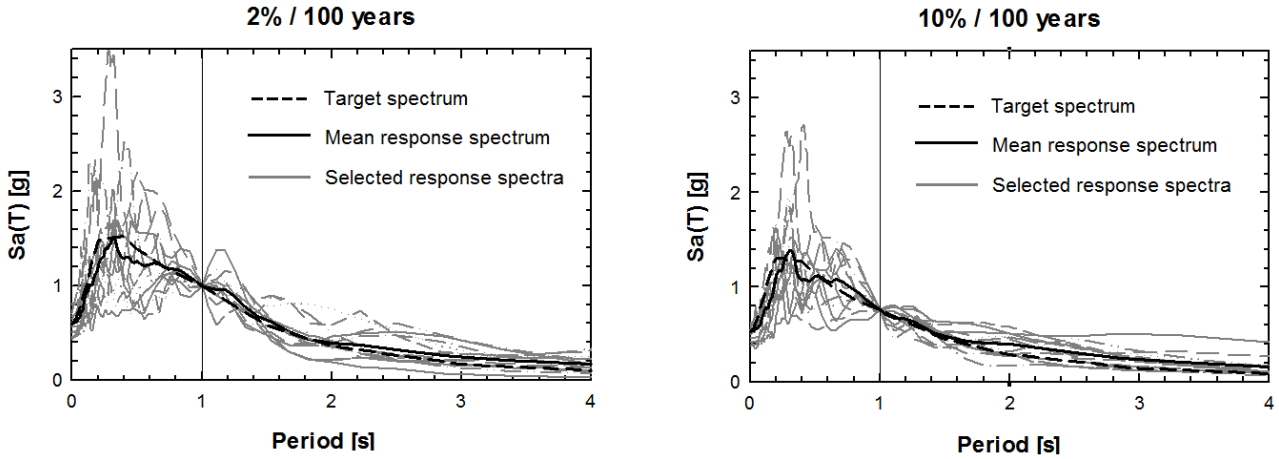
305 Table 1. Spectral acceleration at first-mode period and PGA for each HL.

HL	75%	60%	50%	20%	10%	5%	2%
<b>Sa(<math>T_{ref}</math>) [g]</b>	0.12	0.16	0.20	0.41	0.58	0.76	0.98
<b>PGA [g]</b>	0.17	0.20	0.24	0.38	0.47	0.54	0.62

306

307 The first elastic mode of the building is approximately 1 sec. The related target spectral acceleration  
308 is considered as the IM parameter. Since the structure is regular in plan and elevation, the first period  
309 of the building has been assumed as the reference period ( $T_{ref}$ ). Seven groups of acceleration records  
310 have been selected for each direction and for each HL according to the proposed GMSM procedure.

311 A comparison between the target spectrum and the mean spectrum for HL of 2% and 10% in 100  
 312 years is depicted in Figure 3. The mean spectrum has been obtained as the average of the seven groups  
 313 of spectra also reported in Figure 3. The mean spectrum-compatibility is satisfied into the reference  
 314 range of period.  
 315

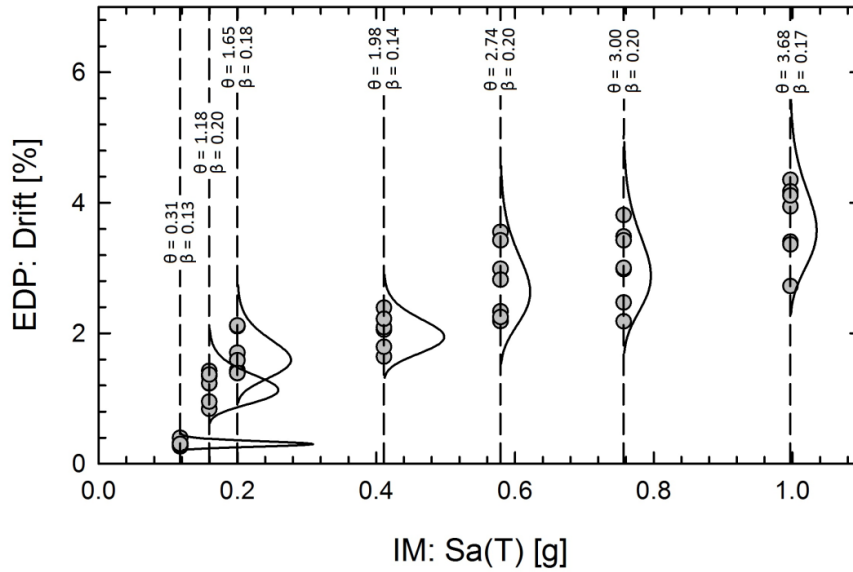


316  
 317 Figure 3. Spectrum-compatibility for 2% and 10% of exceedance probability in 100 years.

318 The spectrum-compatibility criterion is well respected especially for the periods that are close to the  
 319 conditioning period.  
 320

321 *3.3 Analysis of the results and comparison with other GSM methods*

322  
 323 The selected records are the input data of the non-linear analysis. A common approach is to correlate  
 324 the performance of the structure to the maximum inter-story drifts that are capable of providing  
 325 information about the damage state of the elements. Figure 4 indicates the response of the structure  
 326 in terms of maximum drift ratio as EDP values. The response is shown as a function of the spectral  
 327 acceleration at the first period of the structure (IM). The lognormal probability density distribution of  
 328 the structural response has been defined by performing simple statistical analyses. This has been  
 329 conducted by comparing the statistical results in terms of mean ( $\theta$ ) and standard deviation ( $\beta$ ) (Figure  
 330 4).  
 331



332

333

Figure 4. Maximum inter-story drift for each IM and statistical analysis of the results.

334

335

336

337

338

339

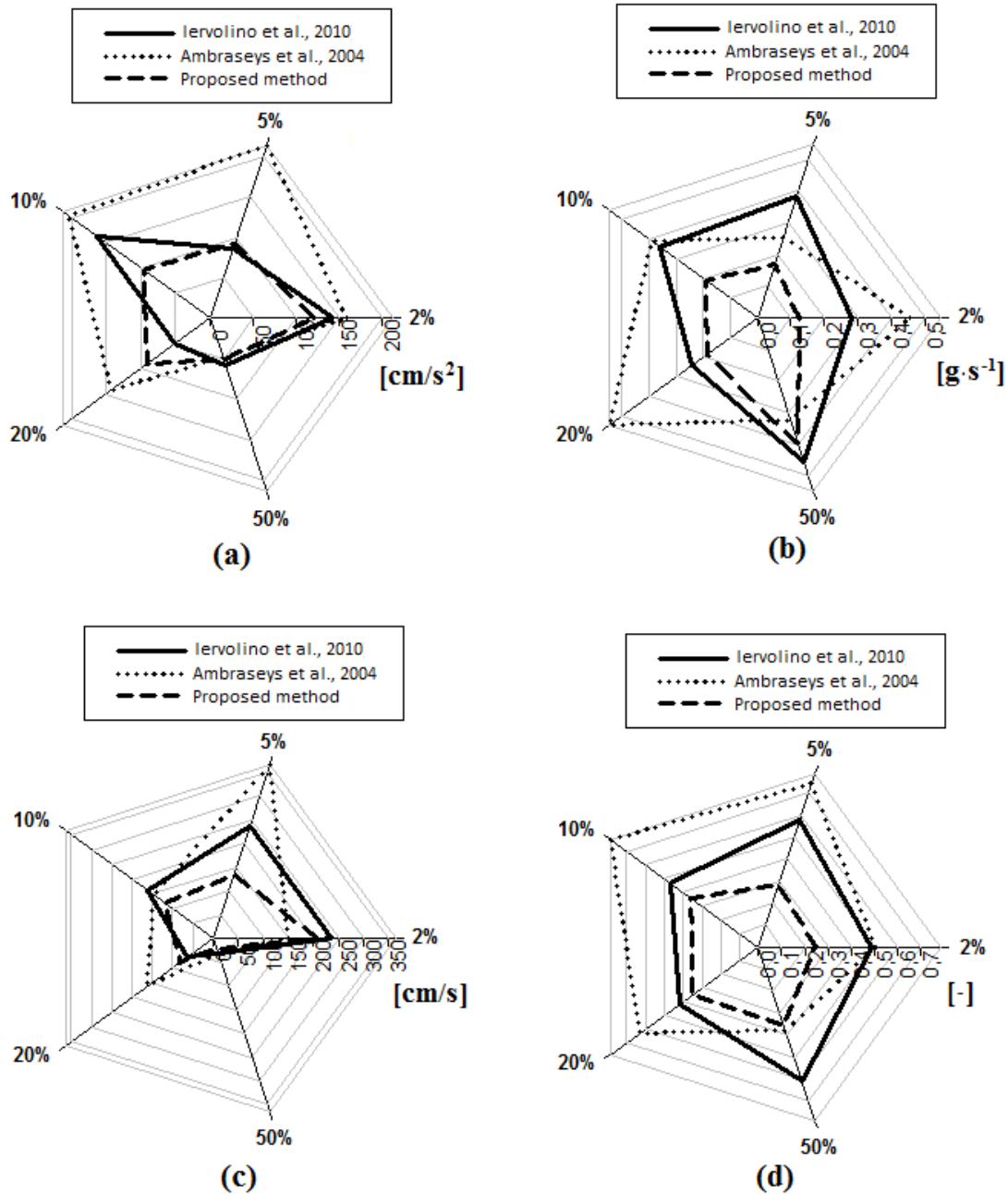
340

341

342

343

For the same structure, the selection procedure has been performed according to the spectrum-compatibility methods proposed by Ambraseys et al. [4] and Iervolino et al. [5]. The spectral acceleration at reference period of the structure has been used as IM and the same seven HLs have been assumed. In order to consistently compare the results, the same ground motion database and range of scale factors have been considered in the selection procedure. For each HL, the records selected using REXEL [5], Ambraseys, and energy-based method have been compared in terms of main ground motion characteristics ( $PGA$ ,  $AV$  ratio, Arias intensity ( $I_A$ ), and structural damage index ( $I_D$ )). Considering the ground motion parameters normally distributed, the mean and standard deviation values have been calculated and compared for HL having exceedance probability greater or equal than 50% in 100 years (Figure 5).

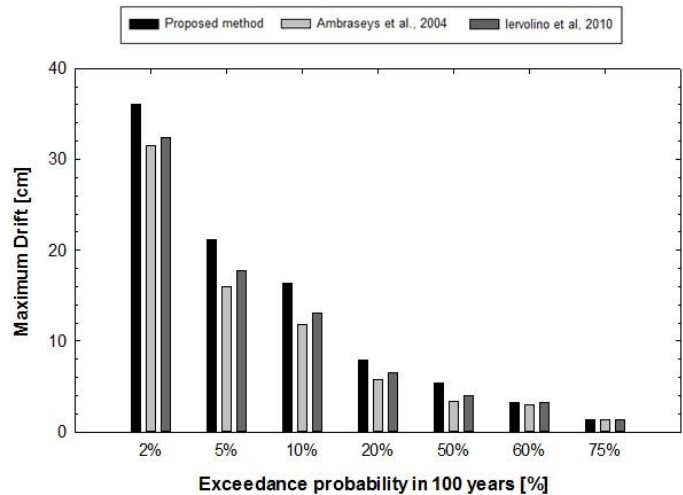
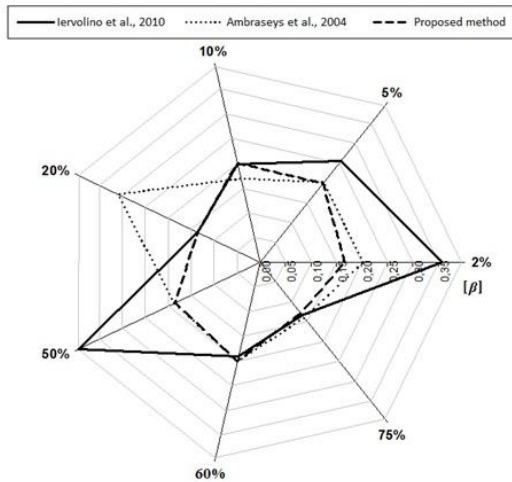


344

345 Figure 5. Comparison of the standard deviation of PGA (a), AV ratio (b),  $I_A$  (c), and  $I_D$  (d) obtained  
 346 through Iervolino et al., 2010 [5], Ambraseys et al., 2004 [4] and the proposed method.

347 The standard deviation of the waveform characteristics gives information about the dispersion of  
 348 these parameters for a given HL (record-to-record variability). The waveform parameters of the  
 349 ground motions selected with the proposed method assume limited values of standard deviation  
 350 compared with the other two considered methods, especially for the structural damage index ( $I_D$ ).  
 351 This is reflected on the structural response by limiting the dispersion of the EDP for a given hazard  
 352 scenario.

353 The records selected through the Ambraseys and Iervolino methods have been used as seismic input  
 354 in the nonlinear dynamic analyses. The results in terms of logarithmic dispersion of maximum inter-  
 355 story drifts ( $\beta$ ) and median maximum inter-story drifts are compared for each HL (Figure 6).

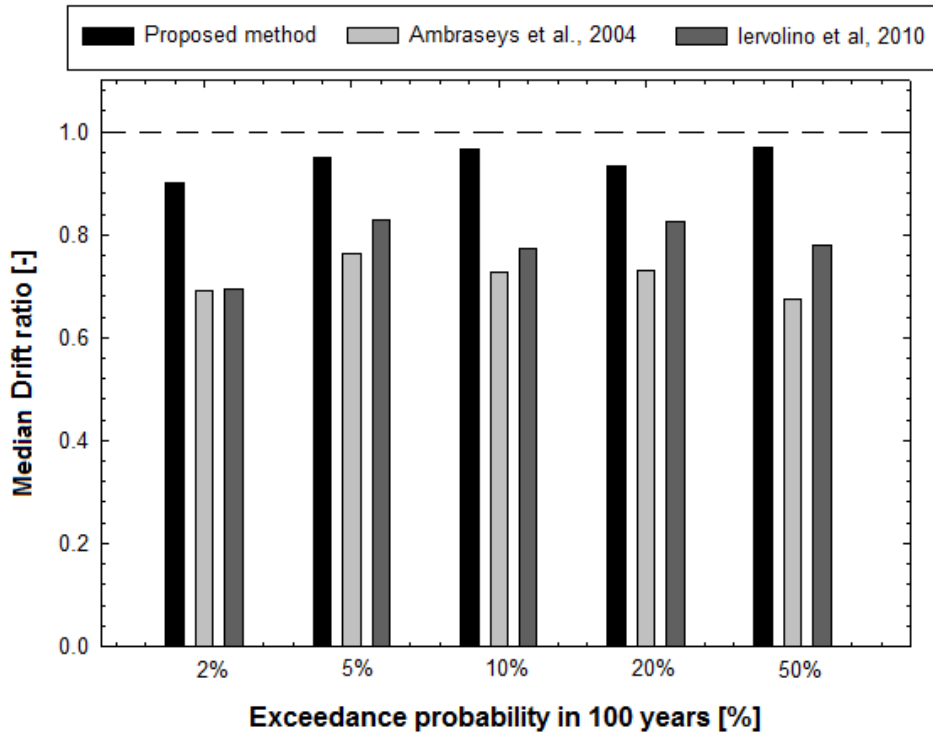


356

357 Figure 6. Comparison of the logarithmic dispersion of maximum inter-story drifts and median  
 358 maximum inter-story drifts obtained through Iervolino et al., 2010 [5], Ambraseys et al., 2004 [4]  
 359 and the proposed method.

360 The proposed method shows a low and uniform dispersion of the EDPs for each HL ( $\beta \leq 0.20$ ) while  
 361 the other two approaches present high dispersion values in some HLs.

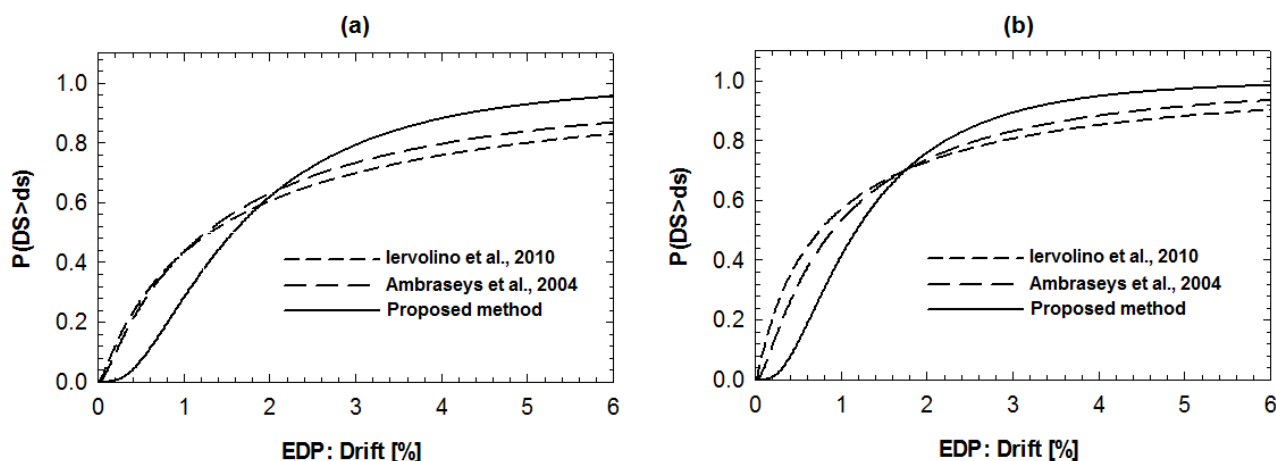
362 According to the definition of Damage States (FEMA 351) [20], the related maximum inter-story  
 363 drifts have been derived for each HL (expected median drifts). Moreover, the ratio between the  
 364 expected median drift and the median drift demand obtained from the time history analyses has been  
 365 evaluated for each HL (median drift ratio). This procedure has been carried out for the ground motions  
 366 selected according to Iervolino, Ambraseys and the proposed method. **Errore. L'origine riferimento  
 367 non è stata trovata.**Figure 7 depicts a comparison of the median drift ratio among the three GSM  
 368 methods.



369

370 Figure 7. Comparison of the median drift ratio obtained through Iervolino et al., 2010 [5],  
 371 Ambraseys et al., 2004 [4] and the proposed method..

372 The full accuracy with the median drift demand for a given hazard scenario is achieved when the  
 373 median drift ratio is equal to one. The median drift ratio resulting from the proposed method is the  
 374 closest to the unit value for each HL. Thus, the proposed method shows an adequate accuracy in  
 375 preserving the median drift demand for a given hazard scenario, especially for high HLs.  
 376 The fragility functions for structural systems are statistical distributions, taking a form of lognormal  
 377 cumulative distribution functions, used to indicate the probability that a component, element, or  
 378 system will be damaged as a function of a given EDP. According to FEMA 351 [20], the extensive  
 379 and complete Damage State (DS) have been identified for the steel building depending on the  
 380 maximum story drift ratio. For each DS, only the drift ratios that do not exceed the associated  
 381 maximum limit have been considered and the related mean and standard deviation have been  
 382 calculated. These statistical parameters have been used to derive the lognormal cumulative  
 383 distribution function that represents the probability to exceed a certain level of damage on the  
 384 considered structure. Figure 8 shows a comparison in terms of fragility functions obtained from the  
 385 three different GSM methods.



386

387 Figure 8. Comparison of the fragility curves obtained through Iervolino et al., 2010 [5], Ambraseys  
 388 et al., 2004 [4] and the proposed method for extensive (a), and complete damage state (b).

389 Since the mean value and the dispersion of structural response influence the estimation of the fragility  
 390 curves, this comparison is of high importance. The fragility curves' dispersions obtained through  
 391 Iervolino and Ambraseys are greater than the dispersion derived from the proposed method.  
 392 Moreover, the mean probability to exceed a certain damage state is about similar for the fragility  
 393 functions resulting from the selection method proposed by Iervolino and Ambraseys. Figure 8 shows  
 394 a difference in terms of mean probability to exceed complete and extensive damage states between  
 395 the proposed method and the Iervolino and Ambraseys methods. This is also reflected in the  
 396 comparison presented in Figure 7.

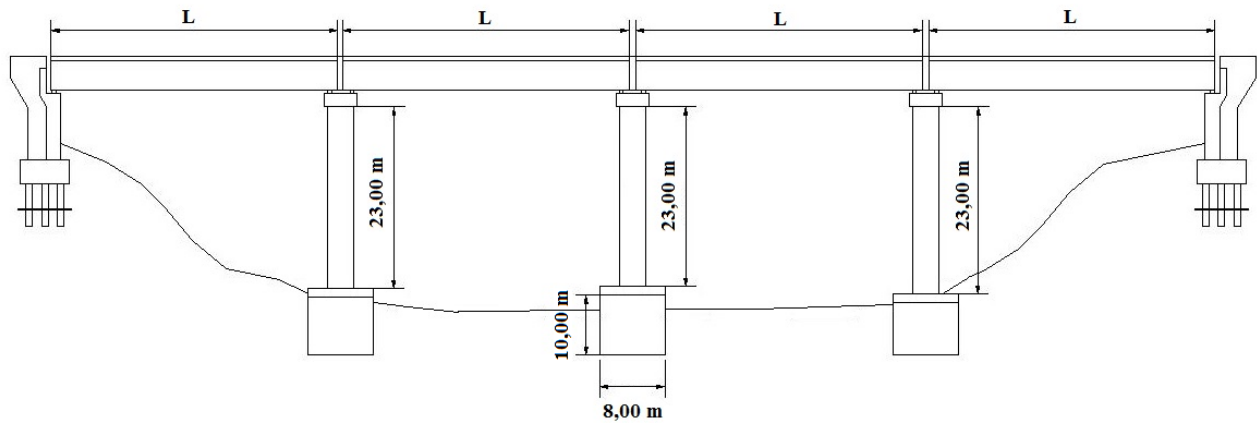
397

#### 398 4 CASE STUDY 2

##### 399 4.1 Description of the structure and structural analysis

400

401 An ordinary reinforced concrete girder bridge located in the city of Savoca, Italy (Lat: 37.9558, Long:  
 402 15.3397) has been investigated. The bridge is composed of four spans with the same length. The three  
 403 internal piers present a full circular cross section with symmetric reinforcement. Each pier has a total  
 404 length of 23 m and rests on a circular shaft foundation that is 10.00 m high and 8.00 m in diameter.  
 405 The foundation soil is a normally consolidated sand with an angle of internal friction of 30° and  
 406 specific weight equal to 20 kN/m<sup>3</sup>. The static scheme of the bridge is showed in Figure 9.



407

408

Figure 9. Static scheme of the case study bridge.

409

410

411

412

413

414

415

416

417

418

419

420

421

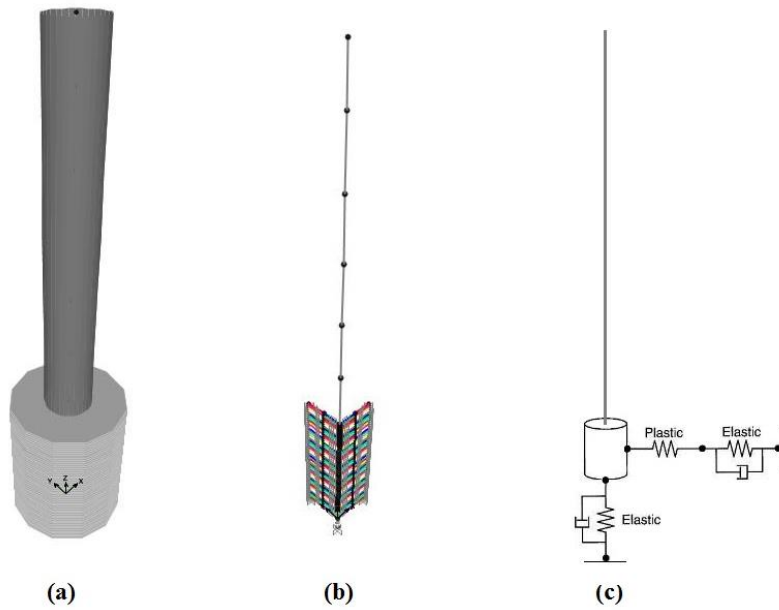
422

423

424

425

The design of the piers has been carried out according to European standards [21][22] while the shaft foundation has been designed and verified according to the Jamiolkowski method [23]. The horizontal soil-structure interaction has been taken into account by modeling the non-linear behavior of the soil and considering a uniform foundation scouring of 1.00 m. According to Boulanger et al [24] and Gerolymus and Gazetas [25] the soil is modeled through macro-elements composed by linear and non-linear elements in series. For the case study, a plastic element and a viscous-elastic element (dashpot-spring model) have been used in series to simulate the soil behavior. The software Sap2000 [14] has been used to model the pier and shaft foundation (model created by Rizzo A.). For the horizontal soil-structure interaction, the *Non-linear-Link* element based on the Wen plastic model has been considered while elastic behavior has been taken into account through the *Linear-Link* element. The force-deformation relationship used to set the non-linear link element has been chosen according to soil characteristic at different depth. The stiffness of the linear link elements has been assessed based on the soil characteristics and assuming for each element a given interaction surface. The vertical soil-structure interaction has been modeled with one *Linear-Link* element connected to the bottom part of the shaft foundation. Figure 10.a depicts an extruded view of the pier connected to the shaft foundation while the associated FEM model is shown in Figure 10.b. In addition, the macro-element model used for the soil-interaction is illustrated in Figure 10.c.



426

427 Figure 10. Extruded view of the structural model (a), FEM model (b) and macro-element model  
 428 used for soil-structure interaction (c).

429 Concentrated plasticity model (CALTRANS type P-M2-M3) has been chosen to consider the  
 430 nonlinearity in the pier. The position of plastic hinge has been supposed coincident with the pier-shaft  
 431 foundation interface, while its length has been assessed according to the Italian standard [26]. The  
 432 non-linear dynamic analyses have been performed taking into consideration the P- $\Delta$  effects and  
 433 applying the horizontal acceleration time histories in the two principal directions of the bridge.

434 *4.2 Ground motion selection and modification*

435

436 Six HLs have been analyzed (i.e., 50%, 20%, 10%, 5%, 2% and 1% of exceedance probability in 50  
 437 years). The Italian Design Response Spectrum (DRS) has been considered as target spectrum [26].  
 438 Further details on the used hazard parameters can be found in the interactive hazard map of INGV  
 439 (<http://esse1-gis.mi.ingv.it/>) [27]. PGA and spectral acceleration at reference period are listed in Table  
 440 2 for each HL.

441

442

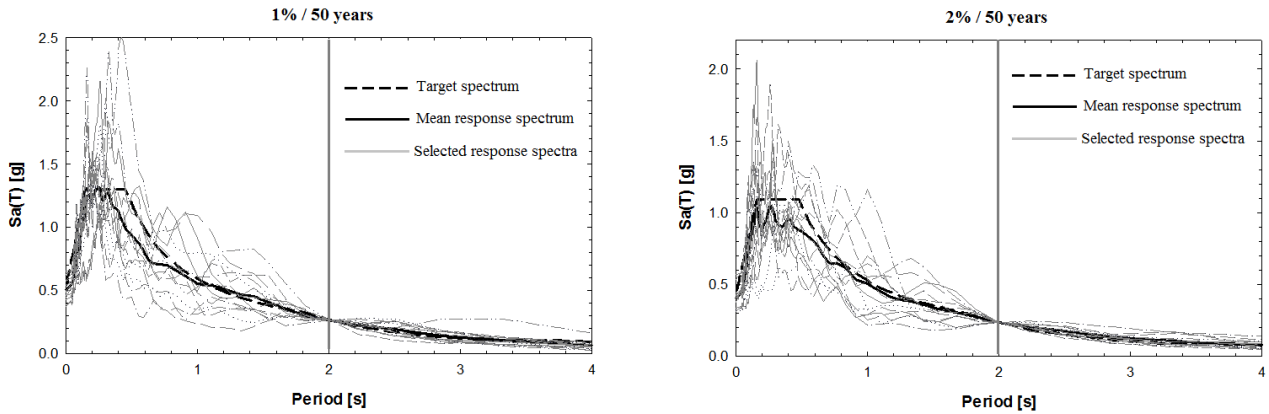
Table 2. Spectral acceleration at first-mode period and PGA for each HLs.

HL	50%	20%	10%	5%	2%	1%
<b>Sa(T<sub>ref</sub>) [g]</b>	0.03	0.06	0.11	0.15	0.24	0.27
<b>PGA [g]</b>	0.10	0.17	0.24	0.30	0.44	0.52

443

444 The fundamental period of the pier, considering the soil-structure interaction, is equal to 1.96 s.  
 445 The related target spectral acceleration is considered as IM parameter. Seven groups of acceleration  
 446 records have been selected for each direction and for each HL according to the proposed GSM  
 447 procedure. The software OPENSIGNAL 4.1 [9] has been used for scaling and selecting ground  
 448 motions. Figure 11 illustrates the mean spectrum compatibility for the cases of 1% and 2% of  
 449 exceedance probability.

450



451

452

Figure 11. Spectrum-compatibility for 1% and 2% of exceedance probability in 50 years.

453

The mean spectra are close to the target spectra within the reference period range.

454

#### 4.3 Analysis of the results and comparison with other GSM methods

455

456

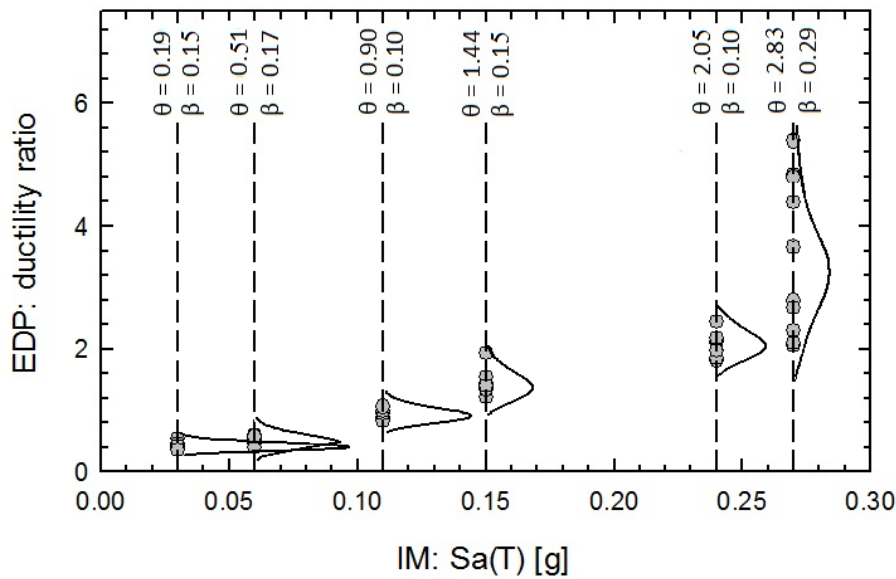
The ductility ratio ( $\mu_d$ ) is considered as EDP to assess the level of damage on the pier. This parameter is defined as the ratio between the maximum plastic top displacement and yielding top displacement of the pier. Since only the structural damage has been assessed, the soil displacement (roto-translation of the shaft foundation) obtained from dynamic non-linear analyses has been removed.

461

The geometric mean of the displacements has been obtained from the non-linear analyses for all the selected records, and the maximum ductility ratios have been considered as EDP. Figure 12 shows the associated values depending on the spectral acceleration at the first period of the pier (IM). Considering the EDPs as lognormally distributed, the mean ( $\theta$ ) and standard deviation ( $\beta$ ) have been calculated for each IM (Figure 12).

466

467



468

469

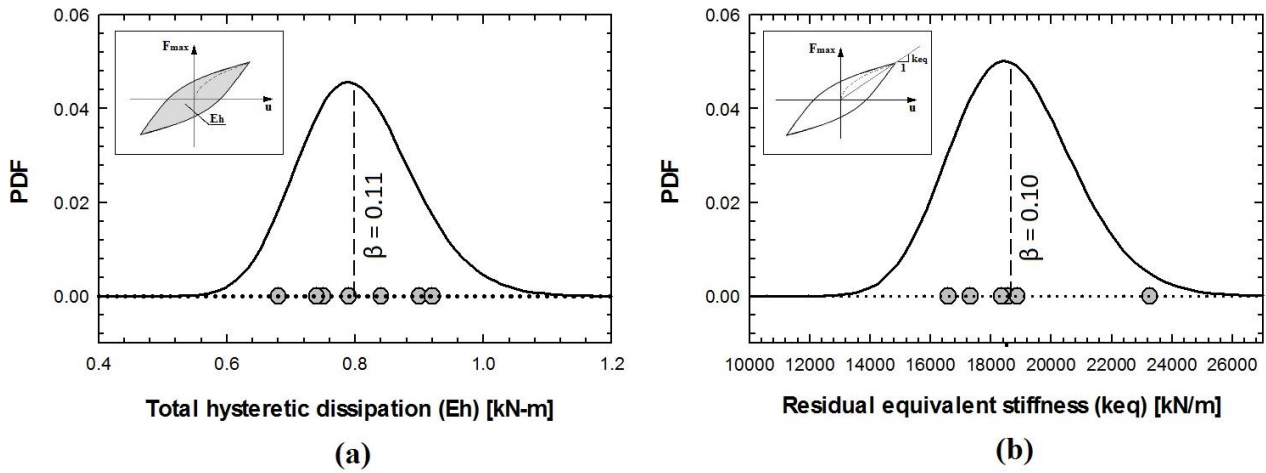
Figure 12. Maximum ductility ratio for each IM and statistical analysis of the results.

470

The dynamic post-elastic soil behavior is influenced by the number of cycles and their amplitude. For high HLs, the degradation of the characteristics of the soil rapidly increases and the soil response is governed by its residual parameters. As an illustrative example, the hysteretic cycles of soil at 2.00

472

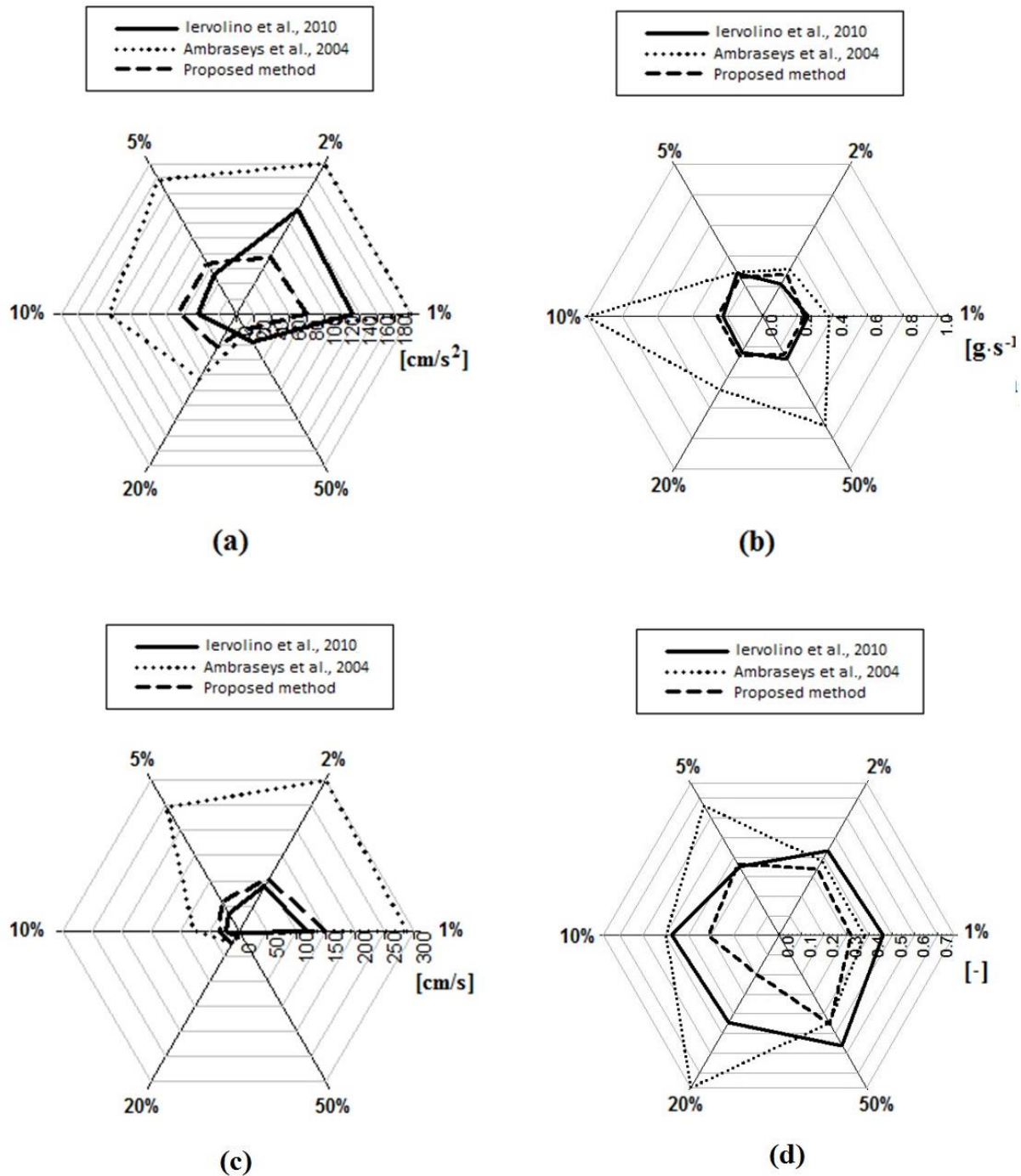
473 m of depth are assessed for HL of 5 % of exceedance probability in 50 years. Figure 13 illustrates the  
 474 lognormal probability density function associated with the total hysteretic dissipation ( $E_h$ ) and the  
 475 residual equivalent stiffness ( $k_{eq}$ ).



476  
 477 Figure 13. Total hysteretic dissipation (a) and residual equivalent stiffness (b) for soil at 2.00 m of  
 478 depth and 5% of exceedance probability in 50 years as HL (The standard deviations  $\beta$  are reported).

479 The total hysteretic dissipation and the residual equivalent stiffness have been considered as soil  
 480 degradation parameters. In both cases, Figure 13 shows a limited dispersion of the results obtained  
 481 from the dynamic non-linear analyses ( $\beta$ ; 0.1).

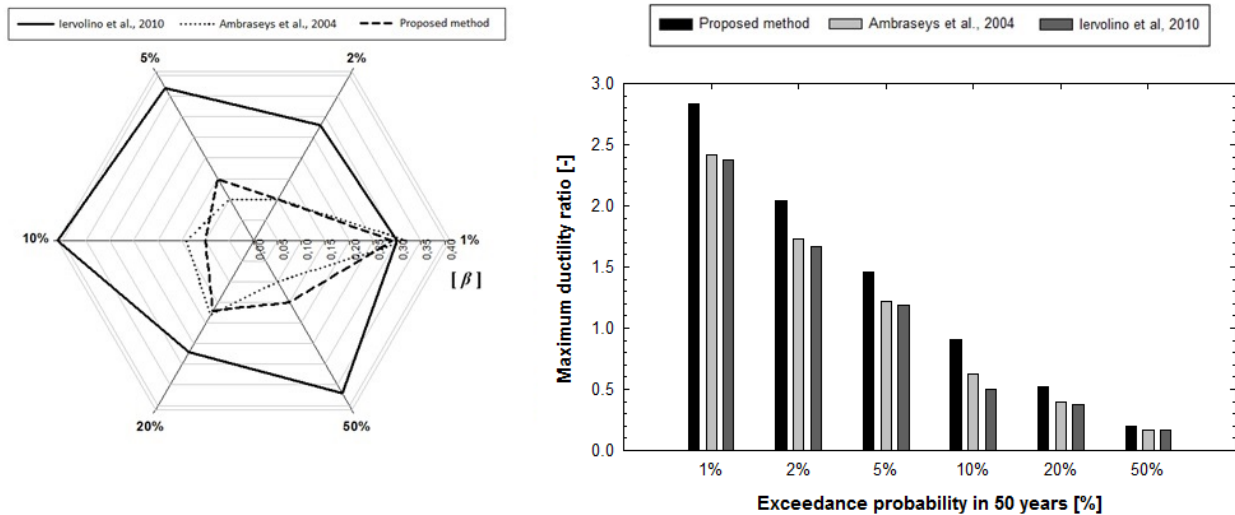
482 The dynamic response of the pier is strongly dependent on the soil behavior, which is sensitive to the  
 483 frequency content of the time histories. Furthermore, the maximum rotation and horizontal  
 484 displacement of the shaft foundation is governed by the total input energy (described by the Arias  
 485 intensity) and on the peak parameters. For each HL, the normal standard deviation of the  $PGA$  and  $I_A$   
 486 resulted by the three considered GSM methods have been compared (Figure 14).



487

488 Figure 14. Comparison of the standard deviation of PGA (a), AV ratio (b), IA (c), and ID (d)  
 489 obtained through Iervolino et al., 2010 [5], Ambraseys et al., 2004 [4] and the proposed method.

490 The energetic-based method allows us to obtain a bounded dispersion of the  $PGA$  and  $I_A$  with  
 491 consequent benefits in terms of stability of the structure-soil response for a given hazard scenario. In  
 492 order to evaluate the uncertainty of the dynamic response of the pier, nonlinear dynamic analyses  
 493 have been performed using the set of motions resulting from Ambraseys and Iervolino method [5].  
 494 Considering the ductile ratio ( $IM$ ) as lognormally distributed for a given hazard scenario, the standard  
 495 deviations values and the median maximum ductility ratios have been assessed and compared (Figure  
 496 15).

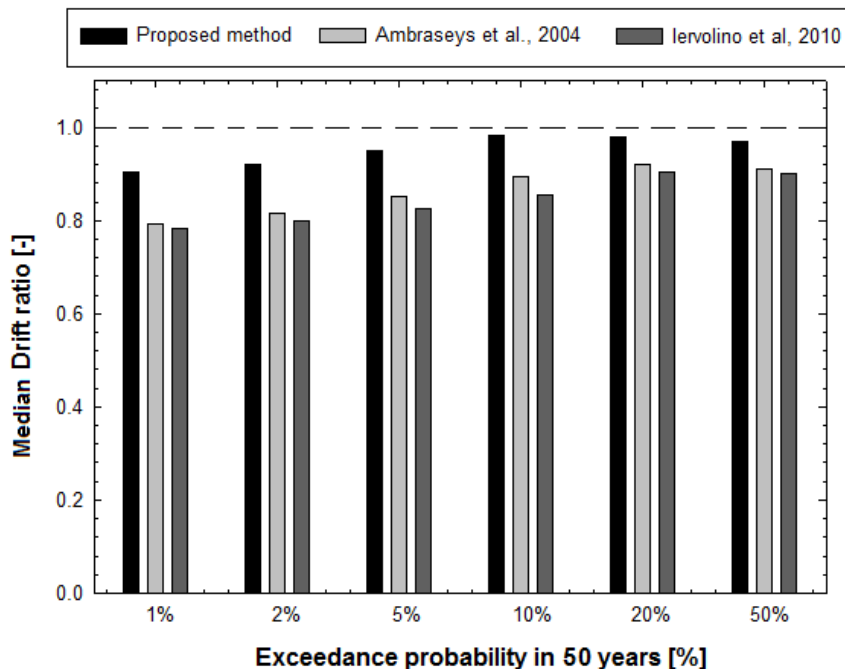


497

498 Figure 15. Comparison of the logarithmic dispersion of maximum ductility ratio and median  
 499 maximum ductility ratio obtained through Iervolino et al., 2010 [5], Ambraseys et al., 2004 [4] and  
 500 the proposed method.

501 Figure 15 shows how the structural dynamic response uncertainty is reduced using the Ambraseys  
 502 and the energetic-based method. In addition, for high hazard scenario (1% of exceedance probability  
 503 in 50 years) the smallest lognormal dispersion of the ductility ratio has been obtained with the  
 504 proposed GSM procedure.

505 A comparison in terms of median drift ratio has been carried out to verify the accuracy in preserving  
 506 the median response for all hazard scenarios (Figure 16).

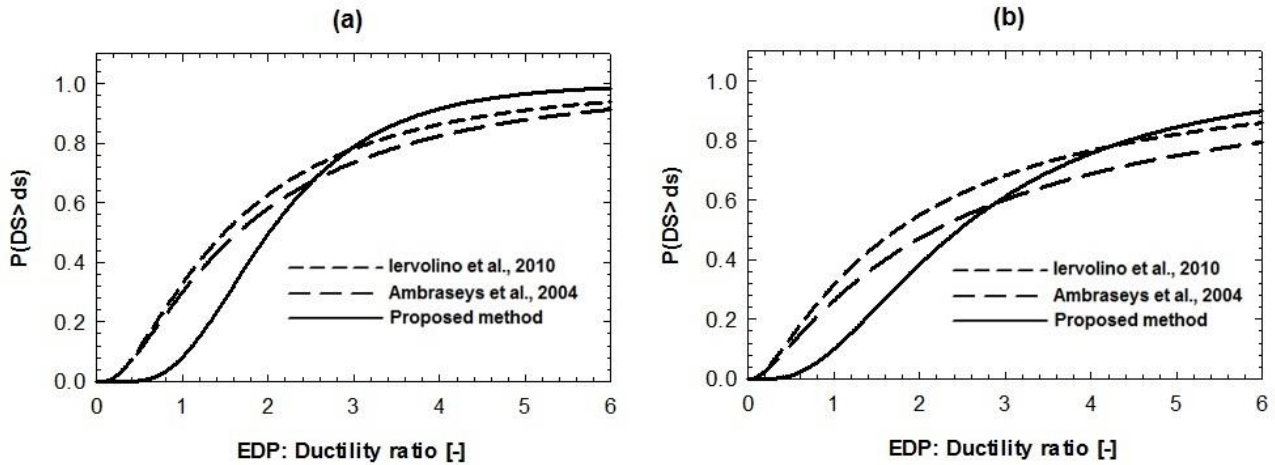


507

508 Figure 16. Comparison of the median drift ratio obtained through Iervolino et al., 2010 [5],  
 509 Ambraseys et al., 2004 [4] and the proposed method.

510 According to the proposed methodology, the median drift ratio is always more representative of the  
 511 median demand for the hazard scenarios. The proposed method is capable of estimating a highly  
 512 representative set of EDPs for each considered hazard scenario.

513 The extensive and complete DS have been considered for the reinforced concrete girder bridge de-  
 514 pending on the maximum ductility ratio. The DS threshold values have been assumed accordingly  
 515 to Banerjee et al. [28] and the fragility functions have been obtained from the three different  
 516 GSM methods (Figure 17).



517  
 518 Figure 17. Comparison of the fragility curves obtained through Iervolino et al., 2010 [5], Ambraseys  
 519 et al., 2004 [4] and the proposed method for extensive (a), and complete damage state (b).

520 The fragility curves' dispersions obtained through Iervolino and Ambraseys are greater than the  
 521 dispersion derived from the proposed method. It is also possible to observe how the mean probability  
 522 to exceed complete and extensive damage states for the proposed method is greater than that one  
 523 obtained through Iervolino and Ambraseys methods. Furthermore, the mean probability to exceed  
 524 complete and extensive damage states obtained with the proposed method is closer to the expected  
 525 one. This is also reflected in the comparison shown in Figure 16.

526

## 527 5 CONCLUSION

528 Currently, the accessibility of ground motion database permits the analysis of structures using real  
 529 ground motion data. Predicting the dynamic behavior of structures is a primary objective; therefore,  
 530 the determination of a set of ground motions that shows a small variability of the structural response  
 531 and accuracy in preserving the median demand is the most challenging task.

532 The new GSM methodology is based on the energy content of the records. It helps in controlling  
 533 the essential variables that influence the dynamic response of structures. In addition, the selected  
 534 records are compatible with the seismic hazard analysis at the site of interest, in terms of the spectral  
 535 acceleration at the period of reference and the M-R parameters. The selected group of ground motion  
 536 records causes an identical elastic seismic action and approximately equal plastic dissipation on the  
 537 structure. The ground motions records have been selected with the main goal of assessing the  
 538 structural response given a certain intensity level. The analysis of the numerical results has shown  
 539 that the selection method significantly affects the structural response estimation and the structural  
 540 damage prediction. The procedure proposed in this work is able to reduce the scatter of the structural  
 541 response parameters around the corresponding mean values and enhance the accuracy in preserving  
 542 the median demand. In addition, the comparisons with other methods have shown the accuracy of the  
 543 estimated median EDPs for every hazard scenario. The accuracy of consequence functions (i.e.,  
 544 casualties, repair time, repair costs, etc.) can be increased by using, in the time history analyses, set  
 545 of motions having low variability and being accurate with the median demand. Therefore, the new

546 GSM procedure can be used to define an earthquake scenario for resilience analyses of a single  
547 building or for a group of buildings.

## 548 ACKNOWLEDGEMENTS

549 The research leading to these results has received funding from the European Research Council under  
550 the Grant Agreement n° ERC\_IDEAL RESCUE\_637842 of the project IDEAL RESCUE—  
551 Integrated Design and Control of Sustainable Communities during Emergencies.

## 552 REFERENCES

- 553 [1] Katsanos EI, Sextos AG, Manolis, GD (2010) Selection of earthquake ground motion records:  
554 A state-of-the-art review from a structural engineering perspective. *Soil Dynamics and*  
555 *Earthquake Engineering* 30, 157–169.
- 556 [2] Applied Technology Council (2011) Draft Guidelines for Seismic Performance Assessment  
557 of Buildings. Volume 1- Methodology ATC-58-1.
- 558 [3] Cornell CA (1968) Engineering Seismic. Risk Analysis. *Bulletin of the Seismological Society*  
559 *of America* 58(5):1583-1606.
- 560 [4] Ambraseys NN, Douglas J, Rinaldis D, Berge-Thierry C, Suhadolc P, Costa G, Sigbjornsson,  
561 R, Smit P (2004) Dissemination of European strong-motion data, vol. 2, CD-ROM collection.  
562 Engineering and Physical Sciences Research Council, UK.
- 563 [5] Iervolino I, Galasso C, Cosenza E (2010) REXEL: computer aided record selection for code-  
564 based seismic structural analysis, *Bull Earthquake Eng* 8:339-362.
- 565 [6] Bradley BA (2010) A generalized conditional intensity measure approach and holistic ground-  
566 motion selection. *Earthquake Engng. Struct. Dyn.* 39: 1321–1342. doi:10.1002/eqe.995
- 567 [7] Shome N, Cornell CA, Bazzurro P, Carballo JE (1998) Earthquakes, records and nonlinear  
568 responses. *Earthquake Spectra*14(3):469-500.
- 569 [8] Baker J, Cornell CA (2006) Spectral shape, epsilon and record selection. *Earthquake*  
570 *Engineering & Structural Dynamics* 35, 1077-1095.
- 571 [9] Cimellaro GP, Marasco S (2015) A computer-based environment for processing and selection  
572 of seismic ground motion records OPENSIGNAL. *Front. Built Environ* 2015; 1:17. DOI:  
573 10.3389/fbuil.2015.00017.
- 574 [10] Cimellaro GP, Reinhorn AM, D'Ambrisi A, De Stefano M . Fragility Analysis and Seismic  
575 Record Selection. *Journal of Structural Engineering*, ASCE, 2011; 137(3), 379-390.
- 576 [11] Cimellaro GP (2013) Correlation in spectral accelerations for earthquakes in Europe.  
577 *Earthquake Engng. Struct. Dyn.* 42(4), 623-633.
- 578 [12] Tso WK, Zhu TJ, Heidebrecht AC (1991) Engineering implication of ground motion A/V  
579 ratio. *Soil Dynamics and Earthquake Engineering* 11 (1992) 133-144.
- 580 [13] Manfredi G (2001) Evaluation of seismic energy demand. *Earthquake Engineering &*  
581 *Structural Dynamics* DOI: 10.1002/eqe.17.
- 582 [14] Computer and Infrastructure Inc. Sap2000, Version 17.3, Berkeley, CA.
- 583 [15] Boore DM, Atkinson GM (2008) Ground-motion prediction equations for the average  
584 horizontal component of PGA, PGV, and 5%-damped PSA at spectral periods between 0.01  
585 s and 10.0 s. *Earthquake Spectra* 24(1), 2008, 99-138.
- 586 [16] USGS. Seismic Hazard Analysis tools. U.S. Geological Survey <  
587 <http://earthquake.usgs.gov/hazards/designmaps/grdmotion.php>>.
- 588 [17] Baker JW (2011) Conditional Mean Spectrum: Tool for Ground-Motion Selection. *Journal of*  
589 *Structural Engineering-Asce* 137, 322-331.
- 590 [18] Lin B, Haselton CB, Baker JW (2013) Conditional-spectrum-based ground motion selection.  
591 Part II: Intensity-based assessments and evaluation of alternative target spectra. *Earthquake*  
592 *Engng. Struct. Dyn.* DOI: 10.1002/eqe.2303.

- 593 [19] Baker JW, Jayaram N (2008) Correlation of spectral acceleration values from NGA ground  
594 motion models. *Earthquake Spectra* 24(1), 299-317.
- 595 [20] FEMA (2000) FEMA 351: Recommended seismic evaluation and Upgrade Criteria for  
596 Existing Welded Steel Moment-Frame Buildings. FEMA 351 Federal Emergency  
597 Management Agency, Federal Emergency Management Agency, Washington D.C.
- 598 [21] EC2 (2002) Design of concrete structures. European Committee for Standardization,  
599 Bruxelles, BG.
- 600 [22] EC8 (2005) Design of structures for earthquake resistance. European Committee for  
601 Standardization, Bruxelles, BG.
- 602 [23] Jamiolkowski M (1968) Atti e rassegna tecnica della società ingegneri e architetti di Torino  
603 n° 7, 169-172 (in Italian).
- 604 [24] Boulanger RW, Curras CJ, Kutter BL, Wilson DW, Abghari A (1999) Seismic soil-pile-  
605 structure interaction experiments and analyses. *Journal of geotechnical and geo-  
606 environmental engineering* 750-759.
- 607 [25] Gerolymos N, Gazetas G (2005) Winkler model for lateral response of rigid caisson  
608 foundations in linear soil, Elsevier 347-361.
- 609 [26] NTC-08 (2008) Nuove Norme Tecniche per le Costruzioni (NTC08). Consiglio Superiore dei  
610 Lavori Pubblici, Ministero delle Infrastrutture, Gazzetta Ufficiale della Repubblica Italiana,  
611 n. 29 (in Italian).
- 612 [27] INGV. The National Institute of Geophysics and Vulcanology. <http://www.ingv.it/en/>.
- 613 [28] Banerjee S, Shinozuka M (2008) Mechanistic quantification of RC bridge damage states under  
614 earthquake through fragility analysis, *Probabilistic Engineering Mechanics* 23.1 (2008): 12-  
615 22.
- 616